




Wound Healing Efficacy of Cellulose Hydrogel in ICR Mice: A Morphoanatomical, Histological, and Genomic Study

Abigail S. Castro^{1,*} , Alvin G. Domingo^{1,2}, Jayon F. Cariaga², Francis A. Gamboa², Aira Cassandra S. Castro⁴, Aira Nadine Q. Pascua¹, Jimmbeth Zenila P. Fabia³, Peter James Icalia Gann^{1,3}, Bjorn S. Santos² and Shirley C. Agrupis^{1,3}

¹Department of Biological Sciences, College of Arts and Sciences, Mariano Marcos State University, City of Batac, Ilocos Norte, Philippines

²National Bioenergy Research and Innovation Center, Mariano Marcos State University, City of Batac, Ilocos Norte, Philippines

³Genomics and Genetic Engineering Laboratory, College of Medicine, Mariano Marcos State University, City of Batac, Ilocos Norte, Philippines

⁴College of Medicine, Mariano Marcos State University, City of Batac, Ilocos Norte, Philippines

Abstract:

Introduction: Chronic wounds pose a significant healthcare challenge due to the risk of infection and the limitations of conventional dressings. Advanced wound care solutions are needed to enhance healing and reduce complications. This study evaluated the wound healing potential of NIMO-CH, a cellulose hydrogel derived from nipa fronds and enriched with nipa indigenous microorganisms, particularly *Lacticaseibacillus paracasei* BCRC-16100.

Methods: 12 male ICR mice with excisional wounds were assigned to three treatment groups: no treatment (negative control), NIMO-CH, and DuoDERM with povidone-iodine (positive control). Wound healing was assessed through macroscopic observation, histological analysis, and genome sequencing of *L. paracasei* BCRC-16100 to determine its potential role in the healing process.

Results: Both NIMO-CH and DuoDERM achieved 100% wound closure. NIMO-CH-treated wounds exhibited complete healing with hair regrowth by days 18–20, whereas untreated wounds healed by day 20. Minimal scarring was observed in both NIMO-CH and DuoDERM groups. Histological analysis revealed comparable healing processes, including granulation tissue formation and moderate inflammatory responses, with no significant differences in collagen fiber orientation. Genome sequencing of *L. paracasei* BCRC-16100 identified the presence of *sodA* and *gsiC* genes, which encode enzymes essential for wound healing.

Conclusion: The findings suggested NIMO-CH to be an effective alternative for wound care, demonstrating comparable healing efficacy to DuoDERM while promoting hair regrowth and minimal scarring. The presence of beneficial genes in *L. paracasei* BCRC-16100 further supported its potential role in enhancing the wound healing process.

Keywords: Wound healing, Cellulose hydrogel, Probiotics, Histological assessment, *Lacticaseibacillus*, Nipa.

© 2025 The Author(s). Published by Bentham Open.

This is an open access article distributed under the terms of the Creative Commons Attribution 4.0 International Public License (CC-BY 4.0), a copy of which is available at: <https://creativecommons.org/licenses/by/4.0/legalcode>. This license permits unrestricted use, distribution, and reproduction in any medium, provided the original author and source are credited.

*Address correspondence to this author at the Department of Biological Sciences, College of Arts and Sciences, Mariano Marcos State University, City of Batac, Ilocos Norte, Philippines; E-mail: castroxabigail@gmail.com

Cite as: Castro A, Domingo A, Cariaga J, Gamboa F, Castro A, Pascua A, Fabia J, Gann P, Santos B, Agrupis S. Wound Healing Efficacy of Cellulose Hydrogel in ICR Mice: A Morphoanatomical, Histological, and Genomic Study. Open Biotechnol J. 2025; 19: e18740707370638. <http://dx.doi.org/10.2174/0118740707370638250424053824>



Received: November 14, 2024

Revised: February 11, 2025

Accepted: March 07, 2025

Published: April 30, 2025



Send Orders for Reprints to
reprints@benthamscience.net

1. INTRODUCTION

Chronic wounds, wounds that can be extremely hard to heal, remain one of the major challenges in public health, causing severe pain and difficulties. These continue to be a silent epidemic, with the occurrence increasing significantly over the past few years [1]. The prevalence of chronic wounds worldwide is estimated to be between 1.51 and 2.21 cases per 1000 individuals, and these numbers are projected to increase with increasing age [2]. In the United States, approximately 2% of the entire population is affected by chronic wounds, and their adverse impact is felt on a global scale [1].

Moreover, the significant mortality rate associated with non-healing wounds in the Philippines might be attributed to the inability of many patients to afford costly medications. Furthermore, the current wound dressings available in the market fail to address the multifaceted factors that contribute to the healing of chronic wounds. If non-healing wounds are left untreated and not managed properly, they can lead to serious medical issues, including infection, sepsis, limb amputation, severe cases, and even death. Hence, there is a pressing need for a more specialized and innovative approach to the development of wound care products.

Currently, new approaches for treating wounds continue to be highly researched [3]. Among these new approaches is the use of cellulose-based hydrogels, linear polysaccharides that form the main component of the cell walls of plants through physical cross-linking, wherein a polymer network can be linked by multiple hydroxyl groups through hydrogen bonding. Cellulose-based hydrogels have gained increasing attention because of their unique properties and potential applications, including their 3D structure, high water content, biocompatibility with a low risk of inducing acute or chronic inflammation, low toxicity, and ability to deliver drugs and growth factors, which address the shortcomings of conventional dressings [4]. Thus, cellulose-based hydrogels hold great promise as versatile and effective materials for wound healing and are likely to play an increasingly vital role in modern medicine.

Furthermore, the growing focus on medicinal products with natural ingredients may ultimately provide a cost-effective, safe, and non-invasive prevention and cure for these wounds, providing a sustainable and locally sourced solution to address the limited availability of wound dressings in the Philippines. In a recent study conducted by Domingo *et al.* [5], a cellulose hydrogel made from nipa fronds was developed and synthesized. To date, there have been no investigations on the use of nipa hydrogel in the medical field. Thus, to comprehensively understand the potential applications of probiotics integrated into the nipa hydrogel in the medical field and lay the groundwork for future research, a thorough investigation of its ability to promote wound healing is essential.

This study aimed to assess wound healing activity in the wounds of ICR mice treated with a probiotic-based cellulose hydrogel derived from nipa in terms of wound contraction, morphoanatomical assessment, and effectiveness through qualitative histological assessment.

2. METHODS

2.1. Genome Sequencing and Promoter Analysis of *Lactacaseibacillus Paracasei* BCRC-16100

2.1.1. Capillary Sequencing

Genomic DNA (gDNA) from BCRC-1600 was isolated via the Quick-DNA Fungal/Bacterial Miniprep Kit (Zymo Research, USA) following the manufacturer's instructions. The PCR amplicons were purified with AMPure XP beads (cat. no. 163881). One microliter of the purified amplicons was analyzed on a 1% agarose gel and run at 120 V for 45 minutes alongside the Invitrogen 1 kb Plus DNA ladder. Fluorescently labeled chain-terminating ddNTPs were utilized for capillary sequencing. The reaction mixture included the amplicons, corresponding primers, and the ABI BigDye® Terminator v3.1 Cycle Sequencing Kit (cat. no. 4337455). The thermal cycler conditions were as follows: holding at 4°C and 96°C for 1 minute, followed by 25 cycles of 96°C for 10 seconds, 50°C for 5 seconds, 62°C for 4 minutes, and a final holding at 4°C. Ethanol precipitation was used to eliminate unincorporated ddNTPs, excess primers, and primer dimers. Capillary electrophoresis was performed using an ABI 3730xl DNA analyzer with a 50 cm 96-capillary array, POP7 polymer (cat. no. 4393714), and 3730xl data collection software v3.1. Base calling was performed via sequencing analysis software v5.4.

2.1.2. Whole Genome Sequencing

Library preparation was carried out via the TruSeq DNA Nano Kit (Illumina, USA), followed by sequencing on an Illumina MiSeq instrument in a paired-end read format of 2 × 150 bp for 300 cycles at the Philippine Genome Center, Quezon City, Philippines.

2.1.3. Prediction of Promoter Elements

Bioinformatics tools, including BPROM and BLAST, were employed to predict promoter elements involved in gene expression related to the wound-healing activity of BCRC-16100. The upstream regions of these genes were extracted from their whole-genome sequences (WGS) and analyzed via the BPROM platform. The analysis identified potential -10 and -35 promoter boxes, their positions within the submitted sequences, and possible associated transcription factors.

2.2. Production of NIMO-CH

2.2.1. Production of Cellulose Hydrogel from Nipa Frond

The isolation and purification of α -cellulose from nipa fronds followed the methodology outlined by Cariaga *et al.* [6], whereas hydrogel synthesis was carried out according to the procedures established by Domingo *et al.* [5].

2.2.2. Derivatization of Carboxymethyl (CMC) from Cellulose

The synthesis of carboxymethylcellulose (CMC) was performed following the protocol outlined by Asl *et al.* [7]. Nine grams of α -cellulose powder derived from Nipa fronds

was combined with 30 ml of 40% NaOH and 270 ml of isopropanol in a beaker and stirred for 30 minutes at room temperature. Subsequently, 10.8 g of sodium monochloroacetate was added, and the mixture was stirred with a magnetic hot plate stirrer. The beaker was covered with aluminum foil and heated at 55°C for 3 hours while maintaining constant stirring at 1200 rpm. Afterward, the mixture was left to stand to allow separation of the upper and sedimentary phases. The upper phase was discarded, and the sedimentary phase was suspended in 70% methanol and neutralized with glacial acetic acid. Following neutralization, the mixture was filtered and washed five times with 70% ethanol *via* vacuum filtration, and then washed again with absolute methanol and filtered. The resulting CMC was air-dried.

2.2.3. Loading of *Lacticaseibacillus paracasei* into the Formulated Nipa Hydrogel

A pure culture of *Lacticaseibacillus paracasei* was initially inoculated into a 250 mL Erlenmeyer flask containing MRS broth and incubated at 35–37°C for 48 hours until turbidity was observed. Following this, the formulation of the CMC nipa hydrogel was initiated according to the methodology established. A solution containing 7% NaOH, 12% urea, and 81% distilled water was prepared in an Erlenmeyer flask and precooled to -12.6°C. One gram of carboxymethylcellulose was then added to the solution and stirred at 1500 rpm for 10 minutes. The mixture was subsequently centrifuged at 8000 rpm for 20 minutes. After centrifugation, the solution was transferred to a beaker and neutralized with 10% sulfuric acid. The CMC solutions were sterilized by autoclaving, and all glassware was sterilized in a hot air oven at 160°C for 2 hours, followed by 30 minutes of UV treatment. The carbomer powder was also UV-treated before use.

To create a sterile environment and promote the exclusive growth of *L. paracasei*, 50 mL of the CMC solution was aseptically transferred to a beaker placed on a magnetic hot plate stirrer. The carbomer powder was gradually added to the CMC solution with continuous stirring until a smooth, homogeneous mixture was obtained. As gelation commenced, one drop of triethanolamine was introduced, followed by pre-inoculation of 50 mL of MRS broth with *L. paracasei*. Once the desired viscosity was reached, the final solution was transferred to a sterile petri dish and stored at 4°C.

2.3. Collection, Care, and Acclimatization of Experimental Animals

Before animal testing, approval was obtained from the Institutional Animal Care and Use Committee (IACUC) of the university. Once approved, 12 male ICR mice of uniform age of 9–10 weeks and weighing 25–20g were obtained from Mariano Marcos State University-Laboratory Animal Care Facility (MMSU-LACF). Each treatment group consisted of 4 mice, which served as replicates for the study. The mice were randomly assigned to the three different treatment groups to ensure unbiased results.

Most of the available data rely on quantitative measures rather than qualitative analysis, utilizing assessment cri-

teria, such as histological scoring, wound contraction rate, and morpho-anatomical evaluation. The rationale behind this choice is to balance the need for sufficient statistical power to determine differences between treatments within the practical limitations of animal research.

The ICR mice were housed individually in 12x12x10 plastic cages with wire mesh under controlled conditions of 22–25°C, 55–75% humidity, adequate ventilation, and a 12-hour light/dark cycle. Cages were cleaned biweekly with soap and water, following the standard operating procedure for disinfection and cage maintenance at MMSU-LACF. Each mouse received approximately 40 grams of pellets as food, and 15–20 mL of purified water was provided in drinking bottles.

Before the experiment commenced, all the mice were acclimatized for five days under these controlled conditions. During this process, the test animals were given free access to food pellets and water *ad libitum*. No exclusions were made from the experiment since all animals were alive and well. Controlled environmental conditions were maintained throughout the experiment, as previously described. To manage the order of treatments and measurements, the groups were arranged vertically on a four-tier shelf, with the negative control group first, followed by the NIMO-CH group, and the positive control at last. This consistent order was maintained throughout the treatment and measurement process.

2.4. Excision of Wounds in ICR Mice and the Application of Treatments

The wound excision procedure was performed according to the protocols established by Dai *et al.* and Rhea and Dunnwald [8, 9] in their murine exceptional wound healing model, with all surgical interventions performed under sterile conditions. The mice were restrained by gently grasping the base of their tail with the thumb and index finger and then placed on a secure surface, such as a wire cage top or towel. The shoulders of mice were held using the free hand, and the scruff of their neck was grasped near the skull to immobilize it. A light strain on the tail from the little finger ensured stability throughout the process.

Topical anesthesia was applied *via* lidocaine cream before each mouse was shaved at the dorsolumbar region and sterilized with 70% alcohol. Circular full-thickness excision wounds, 2.5 cm wide and 0.2 cm deep, were created by grasping the marked skin with toothed forceps and dissecting it using a surgical blade and pointed scissors.

The day following the excisions, morphoanatomical changes in the wounds were recorded for assessment. The mice were then treated as follows: untreated or negative control (group I), nipa hydrogel loaded with nipa indigenous microorganisms (group II), and a commercial hydrogel wound dressing, DuoDERM® (ConvaTec) with povidone-iodine (group III). Treatments were applied topically *via* a sterile cotton-tipped applicator and spread evenly from the wound bed center outward to a thickness of 5 mm.

2.5. Assessment of Wound Healing Activity

For quantitative assessment, the wounds of the mice were measured to assess the healing rate of the wounds. The area of the wound was measured every two days *via* a Vernier caliper, with millimeters (mm) taken as the unit of measurement. To calculate the reduction in the wound area in the study, the formula proposed by Zhang *et al.* [10] was employed:

Healing rate

$$= \frac{\text{Initial wound diameter (mm)} - \text{Final wound diameter (mm)}}{\text{Initial wound diameter (mm)}} \times 100$$

2.6. Morphoanatomical Assessment of Wounded ICR Mice

The morphoanatomical assessment of the study encompassed two data sheets on the effectiveness of different treatments by morphological assessment and histological examination. For the morphological assessment, the qualitative criteria used in the studies by Tabalbag (2012) and Simpliciano (2012) were adopted to determine the effectiveness of the treatments in healing the wounds of mice. The criteria are provided as follows: A (1) very red, very swollen, and moist; B (2) red, swollen, and moist/presence of pus; C (3) red, slightly swollen, and moist; D (4) swollen and moist/dry; E (5) scar formation and dry surface; and F (6) the presence of hair and complete healing of wounds.

2.7. Histological Assessment of Wounded ICR Mice

The histological examination, on the other hand, was performed and sent to the Mariano Marcos Memorial Hospital and Medical Center's (MMMMH & MC) Department of Pathology and Laboratories in Batac City, Ilocos Norte, for analysis. A histological grading criterion adapted from Sultana *et al.* [11] was also utilized (Table 1).

Table 1. The histological grading criteria for healing were established according to the criteria of Sultana *et al.* [11].

Number	Histological Parameter
1	Amount of granulation tissue (profound-1, moderate-2, scanty-3, absent-4)
2	Inflammatory infiltrate (plenty-1, moderate-2, a few-3)
3	Collagen fiber orientation (vertical-1, mixed-2, horizontal-3)
4	Pattern of collagen (reticular-1, mixed-2, fascicle-3)

2.7.1. Collection of Epidermal Tissue Samples

For the histological assessment, the experimental animals were sacrificed *via* cervical dislocation based on the guidelines for the use of cervical dislocation for rodent euthanasia by the Austin Institutional Animal Care and Use Committee at the University of Texas [12]. First, a mouse was restrained in a normal standing position on a firm flat surface, and the base of the tail was grasped firmly with one hand. Then, a sturdy stick-type pen, a rod-shaped piece of metal, or the thumb and first finger of the other hand were placed against the back of the neck at the

base of the skull. To perform the dislocation, forward and downward pressure was quickly applied with the hand or object restraining the head, while simultaneously exerting backward pressure on the base of the tail. The effectiveness of 43 dislocations was verified by their ability to separate cervical tissues. When the spinal cord was severed, a 2–4 mm space was palpable between the occipital condyles and the first cervical vertebra. After cervical dislocation, the marked wound sites of the ICR mice were collected to evaluate the degree of histological alterations according to the criteria mentioned. A longitudinal 4 mm skin tissue sample was collected from the dorsolumbar surface of each mouse. The remaining carcasses were then placed inside labeled plastic bags and transferred to a suitable animal facility for appropriate disposal.

2.7.2. Preparation of Skin Tissue Samples for Histological Assessment

The preparation of skin tissue samples for histological assessment involved several key stages. Initially, the tissue samples were preserved by fixation in 10% neutral buffered formalin overnight at room temperature to ensure structural integrity. Immediately after collection, all skin tissue samples were sent to the Mariano Marcos Memorial Hospital and Medical Center (MMMMH & MC) Pathology Laboratory for further processing and interpretation.

2.7.3. Statistical Analysis of the Data

The study employed a two-step approach to analyze data on the effectiveness and rate of wound healing in mice across different treatment groups. A weighted mean was first calculated to provide a single, overall average of the replicates. Following the weighted mean, one-way ANOVA was conducted to assess statistically significant differences between the treatment groups. Then, results with significant differences after ANOVA analysis were tested again for pairwise mean comparison using the least significant difference (LSD) test to identify which specific treatment pairs differed from each other.

3. RESULTS

3.1. Genomic Analysis

This study involved promoter analysis to support the utilization of *Lacticaseibacillus paracasei* BCRC-16100 in the hydrogel and determine the promoter elements responsible for the expression of genes linked with the wound-healing properties of *L. paracasei* BCRC-16100. Fig. (1) shows the different transcription frequencies.

The genes *sodA* and *gsiC* encode enzymes necessary for the process of wound healing. The *sodA* gene is typically a single-copy gene in most bacteria and is responsible for a significant portion of superoxide dismutase activity, whereas the *gsiC* gene encodes glutathione peroxidase. Wound healing occurs in three stages: inflammation, proliferation, and maturation. During the initial phase, neutrophils and macrophages are drawn to the injured tissue, where they produce reactive oxygen species (ROS) that have bactericidal effects on foreign substances in the wound. However,

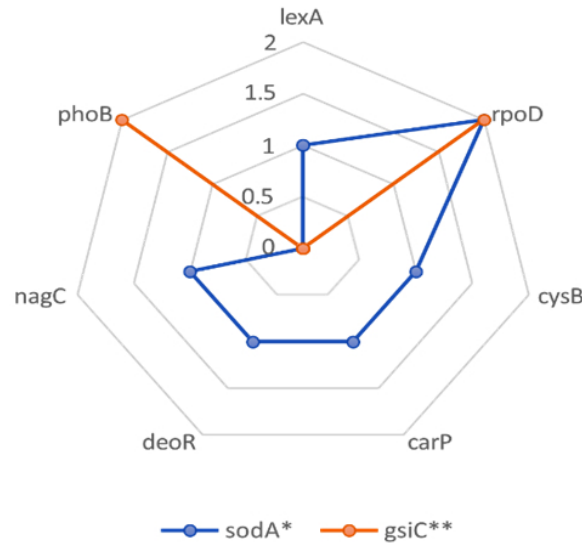


Fig. (1). Transcription frequencies found in BCRC-16100 for skin tissue repair.

excessive ROS can damage tissue and hinder the healing process. Superoxide dismutase and glutathione peroxidase enzymes help neutralize superoxide anions, a type of ROS derived from molecular oxygen. This reduces oxidative stress and creates an environment conducive to cell proliferation and migration, ultimately accelerating tissue repair [13-15].

Although these genes are well-documented, a deeper mechanistic understanding of their specific roles within the context of wound healing and genome analysis requires further investigation. The current study focused only on the wound healing efficacy of the NIMO-CH gel with the incorporation of the *L. paracasei* BCRC-16100, and therefore, a more in-depth analysis of *sodA* and *gsiC* will be pursued in subsequent studies.

The two genes also presented varying transcription frequencies: 7 (*lexA*, *rpoD*, *cysB*, *carP*, *deoR*, *nagC*, and *phoB*) for *sodA* and 4 (*rpoD* and *phoB*) for *gsiC*. The most dominant transcription factor among the two genes identified was *rpoD*, which plays a significant role in coordinating the transcription of the two genes necessary for skin tissue repair.

3.2. Morphoanatomical Assessment

To investigate its potential use for wound healing, NIMO-CH was evaluated in an *in vivo* wound healing model. The weights of the 12 ICR mice were taken before wounding and treatment administration *via* a digital scale. After 21 days of observation, the final weight of each mouse was measured again to test whether weight was a major factor in the wound healing process of the ICR mice. Statistical analysis revealed no significant differences in the mean weights of the experimental animals across the treatment groups, as can be seen in Table 2.

Excisional wounds inflicted on 12 ICR mice were divided into three groups of untreated, NIMO-CH treated, and DuoDERM hydrogel treated with povidone-iodine, for a period of 21 days. Wound diameter was measured every 2 days, along with reapplying the treatments. Morphological changes in the wound bed were observed following the criteria presented in the methodology section (Tables 3, 4).

Table 2. The mean weight of ICR mice before and after the initiation of wounding and treatment.

Treatment Groups	Initial Weight (g)	Final Weight (g)
Untreated (-)	32.30 g	34.72
NIMO-CH	25.80 g	28.52
DuoDERM (+)	29.02 g	29.75
Significance	ns	ns
CV%	13.02	14.24

Note: ns - not significant.

On day 2 of the observation period, all the wounds in the different treatment groups were very red, very swollen, and moist. Blood clots were also observed, following the first stage of wound healing, known as the exudative stage, which may have occurred to prevent bleeding and stop blood loss [16]. On day 4, only the NIMO-CH and positive control groups presented with pus, whereas the negative control group still presented very red and swollen wound beds. The presence of pus is a sign of the inflammatory stage of wound healing. In this stage, mast cells release granules filled with enzymes, histamine, and other active amines that are responsible for characteristic signs of inflammation, such as redness, heat, swelling, and pain, and clear fluid around the cut, which helps clear the wound [17].

On days 6 to 12, redness and swelling around the wound bed slightly decreased in the NIMO-CH and positive control

groups, whereas the negative control group still presented red, swollen, and moist surfaces. Interestingly, wounds in the NIMO-CH group started to dry first, which was followed by the formation of scars on the fourteenth day. This may be likely due to the physiological activity of fibroblasts actively producing collagen and glycosaminoglycans [18]. These components form the foundation of the wound bed, promoting stability and facilitating reepithelialization, which involves the migration of cells from the wound's periphery and adjacent edges. Initially, only a thin superficial layer of epithelial cells is laid down, but a thicker and more durable layer of cells bridges the wound over time, resulting in scar formation.

On day 16, both the untreated group and the positive control group exhibited scar formation. On the eighteenth to twentieth days, the NIMO-CH group presented hair and complete wound healing. On the other hand, the untreated and positive control groups only exhibited complete wound healing by the twentieth day of observation. Final images

were taken, and only minimal scar pigmentation was observed in the NIMO-CH and positive control groups.

Moreover, to further evaluate the effectiveness of NIMO-CH in terms of quantitative data, the healing rates of the different treatment groups were also assessed by measuring the contraction of the wounds of the experimental animals every two days *via* a ruler in millimeters. All wounds involved a diameter of 2.5 cm and a uniform depth. The percentage of wound healing was then calculated *via* the formula described in the methodology section (Table 5).

On day 2, no wound closure was observed across any of the treatment groups. On the fourth day, the NIMO-CH group presented the highest mean percentage of wound closure with a 12% healing rate, followed by the positive control groups with 8% and 2% wound contraction rates. All treatment groups improved steadily over a period of 20 days.

Table 3. Representative pictures of wound progression in ICR mice.

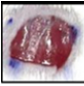

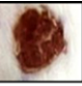
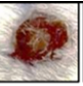
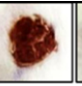
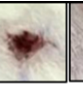
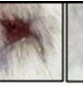
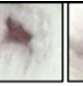


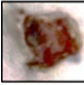

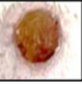

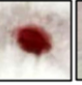
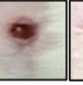

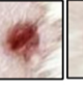
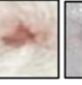






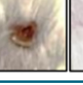

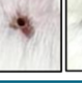


Treatment Groups	Observation Period in Days									
	2	4	6	8	10	12	14	16	18	20
Untreated (-) control										
NIMO-CH										
DuoDERM (+) control										

Table 4. Morphological assessment of the wounds of ICR mice.

Treatment Groups	Observation Period in Days									
	2	4	6	8	10	12	14	16	18	20
Untreated (-) control	A	A	B	B	C	C	D	E	E	F
NIMO-CH	A	B	C	C	C	D	E	E	F	F
DuoDERM (+) control	A	B	C	C	C	D	D	E	E	F

Note: Legend: A (1) Very red, very swollen, and moist, B (2) Red, swollen, and moist/presence of pus, C (3) Red, slightly swollen, and moist, D (4) Swollen and moist/dry, E (5) Scar formation and dry surface, F (6) Presence of hair and complete healing of the wound.

Table 5. Mean percentage (%) of wound healing within the 20-day observation period.

Treatment Groups	Observation Period in Days									
	2	4	6	8	10	12	14	16	18	20
Untreated (-) control	0	2	15	21	60	68	75	80	87	90 ^b
NIMO-CH	0	12	31	47	56	78	86	86	92	100 ^a
DuoDERM (+) control	0	8	31	48	69	78	82	89	94	100 ^a

Note: Legend: * significant at 5% level.

Ns - not significant.

Interestingly, on day 10, the untreated group exhibited a greater percentage of healing than did the NIMO-CH group. This could be due to several factors, such as the initial inflammatory response in the untreated wounds progressed more quickly, leading to a temporary increase in the healing rate in the untreated group. NIMO-CH, on the other hand, might modulate the inflammatory response differently, potentially causing a slight delay in re-epithelialization (skin cell growth) around day 10.

Overall, the healing rates of the NIMO-CH and DuoDERM treatment groups were almost parallel from day 6 onward. By day 20, all the wounds in these two groups had completely healed. The untreated group, on the other hand, did not reach complete healing by the end of day 20, reaching only a 90% wound contraction rate. Statistical analysis revealed that the healing rate from the fourth day to the eighteenth day was not significant, whereas the healing rate from the twentieth day was significant at the 5% level. Moreover, the mean values of both the NIMO-CH and positive control groups were not significantly different from each other.

Furthermore, all the treatments resulted in increased wound healing rates in the ICR mice over time, as evidenced by the increasing trend in their mean percentage of healing. However, it is important to note that the untreated group did not achieve complete healing by day 20, unlike the NIMO-CH and DuoDERM groups (Fig. 2).

3.3. Histological analysis

Monitoring wound progression over time is critical in studies focused on evaluating the efficacy of potential novel therapies, and histological examination of wounds is a very helpful tool to achieve this goal. Therefore, further analysis of the histological features of the wounds in ICR mice was performed after all observations were made. At the end of 21 days, all the ICR mice were sacrificed *via* cervical dislocation, and their skin tissue samples were collected and immediately fixed using 10% formalin in plastic-sealed containers. All samples were sent to MMMH and MC for slide preparation and interpretation.

The wound healing assessment data revealed promising progress across all three treatment groups. In terms of the amount of granulation tissue, all the treatments resulted in consistent and profound amounts of granulation tissue, suggesting robust tissue regeneration. Moderate levels of inflammatory infiltration were also observed across all three treatment groups (Table 6, Fig. 3).

4. DISCUSSION

The findings of this study indicated NIMO-CH loaded with *Lactocaseibacillus paracasei* to have promising potential as an effective wound-healing treatment. Over a 21-day observation period, wound healing progression was monitored across three groups: untreated, NIMO-CH-treated, and DuoDERM hydrogel-treated (positive control).

Mean Percentage Healing of Wounds in ICR Mice

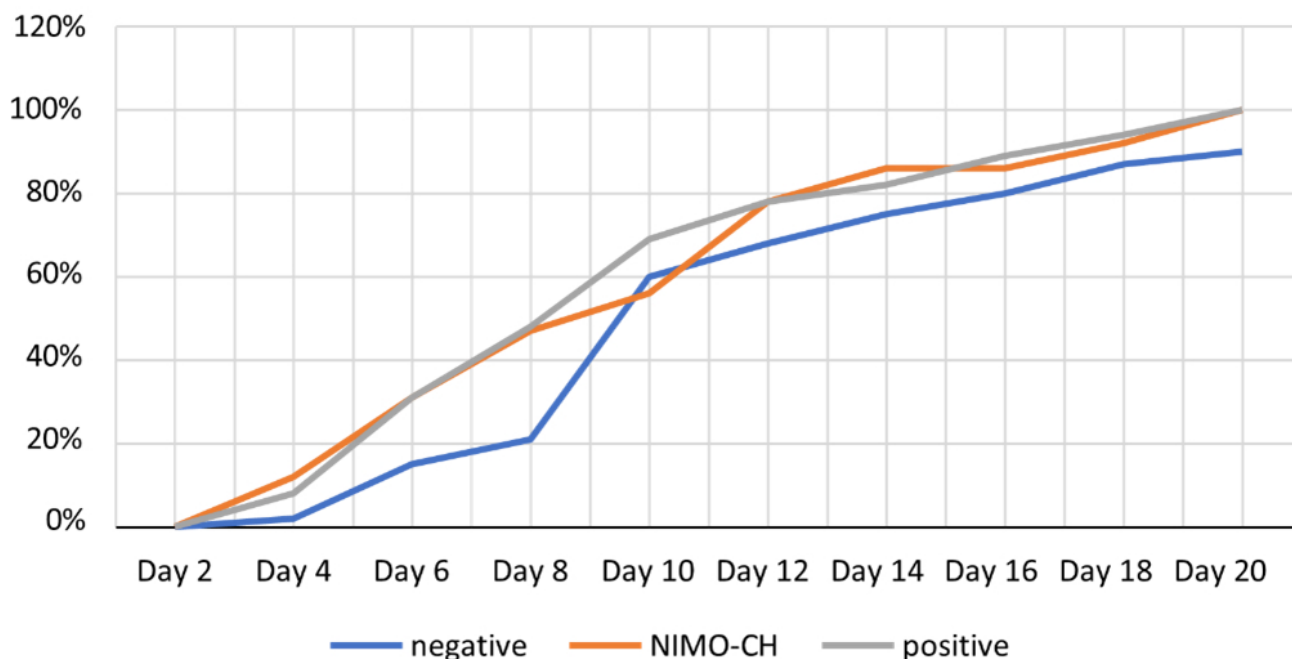


Fig. (2). The trend of the wound contraction rate among the different treatment groups.

Table 6. Results of the histological analysis of the different treatment groups.

Treatment Groups	Mean Score of Histological Parameter				
	Amount of Granulation Tissue	Inflammatory Infiltrate	Collagen Fiber Orientation	Pattern of Collagen	Total Mean Score
Untreated (-) control	4 Absent	3 Few	3 Horizontal	3 Fascicle	13
NIMO-CH	4 Absent	3 Few	2 Mixed	2 Mixed	11
DuoDERM (+) control	4 Absent	3 Few	3 Mixed	3 Mixed	13
Significance	ns	ns	ns	ns	ns
CV %	10.65%	11.76%	22.59%	22.59%	11.58%

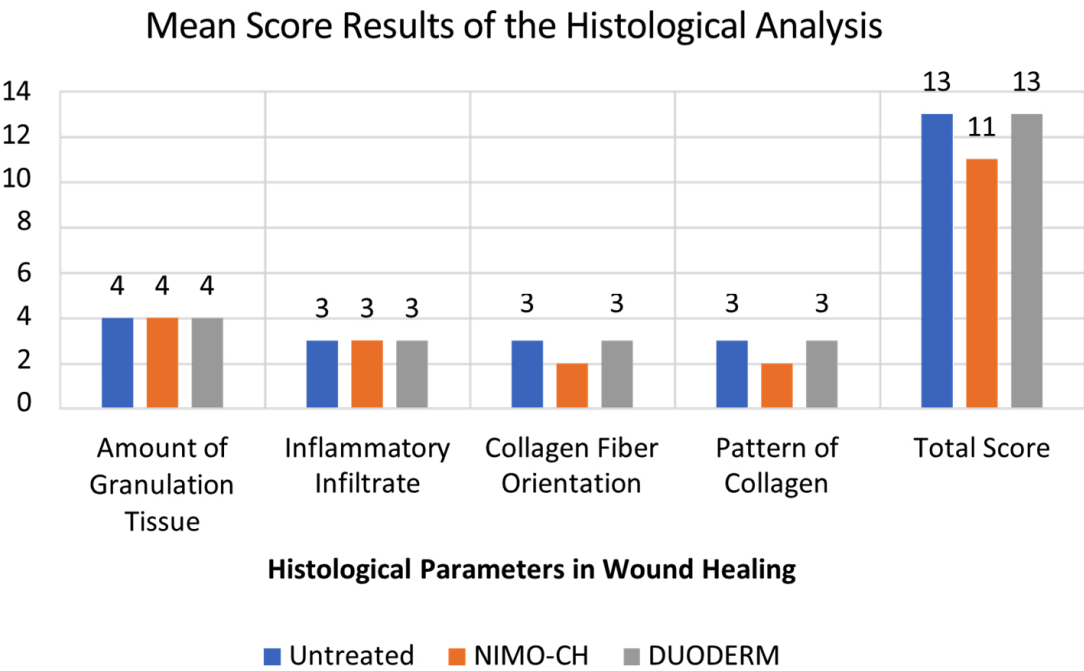


Fig. (3). Graphical representation of the mean score results of the histological analysis.

Statistical analysis revealed that the weight of the mice did not significantly impact the wound-healing process, thereby reinforcing the internal validity of the study and ruling out weight as a confounding variable. Throughout the wound healing stages, the NIMO-CH-treated group effectively progressed, particularly in the exudative, inflammatory, and re-epithelialization stages. This may be due to the genes present, particularly the *soda* and *gsiC* genes in *L. paracasei*, which are responsible for skin tissue repair. This finding has been further supported by the observation that *L. paracasei* SGL15 significantly increased the growth of keratinocytes, which are the main cell types involved in re-epithelialization during wound healing [19]. Compared to DuoDERM-treated wounds, wounds treated with NIMO-CH presented faster scar formation and complete healing by day 20. Both treatments outperformed the untreated wou-

nds, which lagged in terms of wound closure and healing rates, achieving only 90% contraction by day 20.

Histological analysis further supported these findings as all the treatments, including NIMO-CH, promoted the formation of granulation tissue, a critical component in tissue regeneration. Granulation tissue is essential for restoring the skin's dermal layer and orchestrating repair. This complex tissue houses various cell types, extracellular matrix components, and growth factors that orchestrate repair and regeneration [20]. Thus, all three treatments promoted healing *via* the formation of granulation tissue in the dermis. This study did not quantitatively compare the quality, composition, or maturation of this tissue between the treatments administered. Future research should investigate these specific characteristics (*e.g.*, cellularity, vascularity, collagen organization) to elucidate potential differ-

ences in the healing mechanisms elicited by the NIMO-CH group compared to the control groups.

Inflammatory infiltration was also observed at moderate levels in all the treatment groups. The initial stage of wound healing triggers a cascade of immune responses. Neutrophils, macrophages, and lymphocytes recruited from the bloodstream by injury signals infiltrate the wound site [21]. These immune cells not only engulf invading pathogens, but also secrete cytokines and growth factors, promoting tissue repair and initiating the transition to the proliferation stage. The moderate inflammatory infiltration observed in all groups reflected a balanced immune response, as expected during wound healing.

The collagen fiber orientation, which is crucial for the strength and functionality of the healed tissue, showed a mixed pattern across the treatments. A well-organized collagen fiber with a basic network pattern promotes stronger and more functional wound healing, whereas misaligned collagen fibers contribute to scar formation and reduced tissue function [22]. While the presence of a mixed collagen fiber orientation observed in the analysis may suggest some potential for intermediate scarring, the presence of horizontal collagen fibers in certain areas indicated the possibility of stronger wound repair in other areas.

CONCLUSION

In conclusion, the findings of this study showed NIMO-CH to promote wound closure and healing at a rate comparable to the commercially available positive control, DuoDERM. Specifically, wounds treated with NIMO-CH showed faster scar formation and complete healing by day 20, mirroring the performance of DuoDERM, while the untreated group only reached 90% closure by the same time point. This suggests that NIMO-CH facilitated a more efficient and timely repair process.

The effectiveness of NIMO-CH can be attributed, at least in part, to the presence of *L. paracasei* and its associated genes, *sodA* and *gsiC*. These genes encode enzymes superoxide dismutase and glutathione peroxidase, respectively, which are vital for mitigating oxidative stress during the inflammatory phase of wound healing. By neutralizing oxygen, these enzymes create a microenvironment conducive to cell proliferation and migration, which helps the tissue regenerate. The dominant transcription factor, *rpoD*, plays a vital role in coordinating the expression of both *sodA* and *gsiC*, highlighting the intricate regulatory mechanisms underlying the observed wound-healing benefits. Furthermore, the observed increase in keratinocyte growth associated with *L. paracasei* *SGL15* provided additional mechanistic support for the accelerated re-epithelialization observed in the NIMO-CH treated group.

Histological analysis corroborated the macroscopic findings, revealing that NIMO-CH promoted robust granulation tissue formation, a key step in dermal regeneration, comparable to both the positive and negative controls. While all treatments exhibited moderate inflammatory infiltration, indicating a balanced immune response, the collagen fiber orientation in the NIMO-CH group presented a mixed pattern. This observation suggested a potential for

intermediate scarring, though the presence of horizontal fibers within this mixed pattern hinted at areas of potentially stronger wound repair. Further investigation into the specific arrangement and organization of collagen fibers in NIMO-CH treated wounds is warranted to fully elucidate its impact on long-term tissue strength and functionality.

Importantly, statistical analysis revealed no significant differences between NIMO-CH and DuoDERM groups in terms of both wound contraction rates and histological parameters. This equivalent performance underscored the potential of NIMO-CH as a viable and effective alternative to conventional wound care treatments. Its ability to promote timely wound closure, facilitate scar formation, and modulate the inflammatory response, all while exhibiting comparable efficacy to standard-of-care treatment, positions NIMO-CH as a promising candidate for future wound healing applications. Further research, including clinical trials, is necessary to fully evaluate its safety and efficacy in human patients and optimize its formulation for clinical use.

AUTHORS' CONTRIBUTIONS

The authors confirm their contribution to the paper as follows: A.D.: Study conception and design; F.G.: Data collection; A.N.P., B.S.: Data curation; S.A.: Supervision and funding acquisition; P.J.G.: Investigation; J.Z.F.: Validation; A.C.C.: Analysis and interpretation of results; A.C.: Drafting of the manuscript; J.C.: Methodology. All authors have reviewed the results and approved the final version of the manuscript.

LIST OF ABBREVIATIONS

NIMO-CH	= Nipa Indigenous Microorganisms - Cellulose Hydrogel
WGS	= Whole-genome Sequences
CMC	= Carboxymethylcellulose
IACUC	= Institutional Animal Care and Use Committee
MMMH & MC	= Mariano Marcos Memorial Hospital and Medical Center
ROS	= Reactive Oxygen Species

ETHICS APPROVAL AND CONSENT TO PARTICIPATE

The ethical approval was obtained from the Institutional Animal Care and Use Committee (IACUC) of the university. Protocol Approval with study protocol no. 2023-002. Animal Research Clearance was also obtained from the Department of Agriculture - Bureau of Animal Industry, Philippines with reference number AR-2024-0151.

HUMAN AND ANIMAL RIGHTS

The reported experiments were in accordance with the Guide for the Care and Use of Laboratory Animals. This study adhered to internationally accepted standards for animal research, following the 3Rs principle. The ARRIVE guidelines were employed for reporting experiments involving live animals, promoting ethical research practices.

CONSENT FOR PUBLICATION

Not applicable.

AVAILABILITY OF DATA AND MATERIALS

The data and supportive information are available within the article.

FUNDING

This research study was funded by Mariano Marcos the National Bioenergy Research and Innovation Center (NBRIC), Philippines.

CONFLICT OF INTEREST

The authors declare no conflict of interest, financial or otherwise.

ACKNOWLEDGEMENTS

Declared none.

REFERENCES

- [1] Järbrink K, Ni G, Sönnnergren H, *et al.* Prevalence and incidence of chronic wounds and related complications: A protocol for a systematic review. *Syst Rev* 2016; 5(1): 152.
<http://dx.doi.org/10.1186/s13643-016-0329-y> PMID: 27609108
- [2] Martinengo L, Olsson M, Bajpai R, *et al.* Prevalence of chronic wounds in the general population: Systematic review and meta-analysis of observational studies. *Ann Epidemiol* 2019; 29: 8-15.
<http://dx.doi.org/10.1016/j.annepidem.2018.10.005> PMID: 30497932
- [3] Yaseen HS, Asif M, Saadullah M, *et al.* Methanolic extract of *Ephedra ciliata* promotes wound healing and arrests inflammatory cascade *in vivo* through downregulation of TNF- α . *Inflammopharmacology* 2020; 28(6): 1691-704.
<http://dx.doi.org/10.1007/s10787-020-00713-7> PMID: 32385747
- [4] Jose G, Shalumon KT, Chen J-P, Yu C. Natural polymers based hydrogels for cell culture applications. *Curr Med Chem* 2019; 26: 3004.
<http://dx.doi.org/10.2174/0929867326666190903113004> PMID: 31480996
- [5] Domingo AG, Cariaga JF, Santos BS, Agrupis SC. Production of cellulose hydrogel from Nipa (*Nypa fruticans* Wurmb) frond. *Indian J Sci Technol* 2023; 16(20): 1487-94.
<http://dx.doi.org/10.17485/IJST/v16i20.2336>
- [6] Cariaga JF, Domingo AG, Santos BS, Agrupis SC. Isolation of a -cellulose from nipa (*Nypa fruticans* wurmb) frond using physico-chemical treatment. *Indian J Sci Technol* 2023; 16(23): 1754-9.
<http://dx.doi.org/10.17485/IJST/v16i23.2258>
- [7] Alizadeh Asl S, Mousavi M, Labbafi M. Synthesis and characterization of carboxymethyl cellulose from sugarcane bagasse. *J Food Process Technol* 2017; 8(8): 1000687.
<http://dx.doi.org/10.4172/2157-7110.1000687>
- [8] Dai T, Kharkwal GB, Tanaka M, Huang YY, Bil de Arce VJ, Hamblin MR. Animal models of external traumatic wound infections. *Virulence* 2011; 2(4): 296-315.
<http://dx.doi.org/10.4161/viru.2.4.16840> PMID: 21701256
- [9] Rhea L, Dunnwald M. Murine excisional wound healing model and histological morphometric wound analysis. *J Vis Exp* 2020; 162: 10.
<http://dx.doi.org/10.3791/61616>
- [10] Zhang W, Yang Z, Zhang M, *et al.* A hybrid hydrogel constructed using drug loaded mesoporous silica and multiple response copolymer as an intelligent dressing for wound healing of diabetic foot ulcers. *J Mater Chem B Mater Biol Med* 2023; 11(22): 4922-33.
<http://dx.doi.org/10.1039/D3TB00395G> PMID: 37194321
- [11] Sultana J, Molla MR, Kamal M, Shahidullah M, Begum F, Bashar MA. Histological differences in wound healing in Maxillofacial region in patients with or without risk factors. *Bangladesh J Pathol* 1970; 24(1): 3-8.
<http://dx.doi.org/10.3329/bjpath.v24i1.2874>
- [12] Policies, guidelines and forms. 2024. Available from: <https://research.utexas.edu/resources/animal-care/policies-procedures> (accessed on 17-3-2024).
- [13] Jair HW, Lu HF, Huang YW, *et al.* Roles of the Two-MnSOD system of *Stenotrophomonas maltophilia* in the alleviation of superoxide stress. *Int J Mol Sci* 2019; 20(7): 1770.
<http://dx.doi.org/10.3390/ijms20071770> PMID: 30974814
- [14] Iuchi Y, Roy D, Okada F, *et al.* Spontaneous skin damage and delayed wound healing in SOD1-deficient mice. *Mol Cell Biochem* 2010; 341(1-2): 181-94.
<http://dx.doi.org/10.1007/s11010-010-0449-y> PMID: 20352474
- [15] Comino-Sanz IM, López-Franco MD, Castro B, Pancorbo-Hidalgo PL. The role of antioxidants on wound healing: A review of the current evidence. *J Clin Med* 2021; 10(16): 3558.
<http://dx.doi.org/10.3390/jcm10163558> PMID: 34441854
- [16] Wang C, Wang M, Xu T, *et al.* Engineering bioactive self-healing antibacterial exosomes hydrogel for promoting chronic diabetic wound healing and complete skin regeneration. *Theranostics* 2019; 9(1): 65-76.
<http://dx.doi.org/10.7150/thno.29766> PMID: 30662554
- [17] Schultz GS, Chin GA, Moldawer L, Diegelmann RF. Principles of Wound Healing. University of Adelaide Press 2011.
- [18] Wallace H, Basehore B, Zito P. Wound Healing Phases. Statpearls. Treasure island: Statpearls Publishing 2023.
- [19] Brandi J, Cheri S, Manfredi M, *et al.* Exploring the wound healing, anti-inflammatory, anti-pathogenic and proteomic effects of lactic acid bacteria on keratinocytes. *Sci Rep* 2020; 10(1): 11572.
<http://dx.doi.org/10.1038/s41598-020-68483-4> PMID: 32665600
- [20] Plikus MV, Guerrero-Juarez CF, Ito M, *et al.* Regeneration of fat cells from myofibroblasts during wound healing. *Science* 2017; 355(6326): 748-52.
<http://dx.doi.org/10.1126/science.aai8792> PMID: 28059714
- [21] Wang Z, Qi F, Luo H, Xu G, Wang D. Inflammatory microenvironment of skin wounds. *Front Immunol* 2022; 13: 789274.
<http://dx.doi.org/10.3389/fimmu.2022.789274> PMID: 35300324
- [22] Su CY, Liu TY, Wang HV, Yang WC. Histopathological study on collagen in full-thickness wound healing in Fraser's dolphins (*Lagenodelphis hosei*). *Animals (Basel)* 2023; 13(10): 1681-1.
<http://dx.doi.org/10.3390/ani13101681> PMID: 37238111